Quasi-two-dimensional Fermi surfaces in the flat antiferromagnetic Brillouin zone of $NpRhGa_5$ studied by dHvA experiments and energy band calculations

2005 J. Phys.: Condens. Matter 17 L169

(http://iopscience.iop.org/0953-8984/17/17/L03)

INSTITUTE OF PHYSICS PUBLISHING JOURNAL OF PHYSICS: CONDENSED MATTER

J. Phys.: Condens. Matter **17** (2005) L169–L175 doi:10.1088/0953-8984/17/17/L03

LETTER TO THE EDITOR

Quasi-two-dimensional Fermi surfaces in the flat antiferromagnetic Brillouin zone of $NpRhGa_5$ studied by dHvA experiments and energy band calculations

Dai Aoki[1], Hiroshi Yamagami[2], Yoshiya Homma[1], Yoshinobu Shiokawa[1,3], Etsuji Yamamoto[3], Akio Nakamura[3], Yoshinori Haga[3], Rikio Settai[4] and Yoshichika Ōnuki[3,4]

[1] Institute for Materials Research, Tohoku University, Oarai, Ibaraki 311-1313, Japan
[2] Department of Physics, Faculty of Science, Kyoto Sangyo University, Kyoto 603-8555, Japan
[3] Advanced Science Research Center, Japan Atomic Energy Research Institute, Tokai, Ibaraki 319-1195, Japan
[4] Graduate School of Science, Osaka University, Toyonaka, Osaka 560-0043, Japan

E-mail: aoki@imr.edu

Received 1 March 2005
Published 15 April 2005
Online at stacks.iop.org/JPhysCM/17/L169

Abstract

We succeeded in growing a high-quality single crystal of $NpRhGa_5$ by the Ga-flux method and observed the de Haas–van Alphen oscillation in the antiferromagnetic state. Four kinds of nearly cylindrical Fermi surfaces, which correspond to main Fermi surfaces, were clearly detected. These quasi-two-dimensional Fermi surfaces are formed in the flat antiferromagnetic Brillouin zone and are well explained on the basis of spin- and orbital-polarized LAPW energy band calculations. The cyclotron masses are moderately enhanced, ranging from 8.1 to 11.7 m_0, which are approximately four times larger than the corresponding band masses. This is the first case where the 5f-itinerant band model is applicable to a neptunium magnetic compound.

The recent discovery of superconductivity in $PuCoGa_5$ and $PuRhGa_5$ with a superconducting transition temperature $T_c = 18.5$ and 8 K, respectively, has provided a perspective on new physics for the transuranium compounds with 5f electrons [1, 2]. Three kinds of cylindrical Fermi surfaces are calculated on the basis of the 5f-itinerant band model [3, 4]. However, the localized 5f-electron picture might be applicable at high temperatures, because the magnetic susceptibility follows the Curie–Weiss law with an effective moment expected for Pu^{3+}. It is important to clarify the electronic states experimentally in the transuranium compounds including Pu and Np. Nevertheless, there are no reports on de Haas–van Alphen (dHvA) experiments to clarify the Fermi surface properties for these compounds, because it is very

difficult to treat them experimentally due to the high radioactivity and requirements of special equipment and techniques.

Recently we observed the dHvA oscillations in $NpNiGa_5$ [5] and $NpCoGa_5$ [6] for the first time in transuranium compounds. $NpNiGa_5$ undergoes ferromagnetic ordering at a Curie temperature $T_C = 30$ K and becomes a canted magnet below $T^* = 18.5$ K [7, 8]. We detected the main dHvA branches in $NpNiGa_5$ but could not determine the topology of the Fermi surfaces because of the complicated magnetism.

On the other hand, $NpCoGa_5$ is a very simple antiferromagnet with a Néel temperature $T_N = 47$ K and an ordered moment $\mu_s = 0.8\ \mu_B$/Np [9, 10]. The antiferromagnetic moments are oriented along the [001] direction of the $HoCoGa_5$-type tetragonal crystal structure with the propagation vector $\boldsymbol{q} = (0\,0\,1/2)$. Namely, the magnetic moments of Np are aligned ferromagnetically in the (001) plane, and are stacked along [001] in an antiferromagnetic ($\uparrow\downarrow$) sequence. This means that the magnetic unit cell is doubled with respect to the chemical unit cell. In the magnetization measurements, a sharp metamagnetic transition was found at $H_m = 43$ kOe for $H \parallel [001]$, where the antiferromagnetic state changes into the field-induced ferromagnetic state above H_m [11]. Two kinds of nearly cylindrical Fermi surfaces were detected in the field-induced ferromagnetic state, namely at high magnetic fields $H > H_m$ via the dHvA experiments [6].

$NpRhGa_5$ is also an antiferromagnet with the same crystal structure. According to recent reports on Mössbauer [12] and neutron scattering experiments [13], an antiferromagnetic transition occurs at $T_{N1} = 37$ K and it undergoes a second magnetic transition below $T_{N2} = 32$ K. The magnetic structure in the temperature range from T_{N1} to T_{N2} is the same as that in $NpCoGa_5$, but a reorientation of the magnetic moment from the [001] direction to [110] occurs at $T_{N2} = 32$ K. The ordered moment of Np is determined as $\mu_s = 0.96\ \mu_B$/Np [12] and the antiferromagnetic propagation vector is thus $\boldsymbol{q} = (0\,0\,1/2)$ below T_{N1}, which is unchanged even below T_{N2} [13]. The magnetic structure of $NpRhGa_5$ is thus very similar to that of $NpCoGa_5$ except for the direction of the ordered moment. Therefore $NpCoGa_5$ is a good reference compound for the Fermi surface study of $NpRhGa_5$.

In the present letter, we report the observed quasi-two-dimensional Fermi surfaces determined from dHvA experiments in the antiferromagnetic state of $NpRhGa_5$. The obtained Fermi surfaces are discussed on the basis of the spin- and orbital-polarized LAPW energy band calculations, indicating that the 5f-itinerant band model can be applied to the neptunium magnetic compound. These studies are the first case in the transuranium compounds.

The Np metal was obtained from NpO_2 by the electrolysis of an aqueous solution [14]. The single crystals of $NpRhGa_5$ were grown by the Ga-flux method [11]. We have characterized the sample by measuring the electrical resistivity and specific heat. The resistivity shows a clear kink at $T_{N1} = 36$ K and a steep drop below $T_{N2} = 32$ K [7]. The residual resistivity ρ_0 and residual resistivity ratio RRR ($\equiv \rho_{RT}/\rho_0$) were 3.01 $\mu\Omega$ cm and 141, respectively, indicating the high quality of the present sample. No superconductivity was observed at temperatures down to 0.6 K. A very sharp jump in the specific heat, which was most likely of the first order transition, was observed at $T_{N2} = 32$ K, and a λ-type anomaly was observed at $T_{N1} = 36$ K. The electronic specific heat coefficient γ was obtained as 52 mJ K^{-2} mol^{-1}.

To clarify the Fermi surface properties of $NpRhGa_5$, we have carried out the dHvA experiments by the standard field modulation method at temperatures down to 25 mK and in the magnetic field range between 60 and 150 kOe for all field directions, where $NpRhGa_5$ is in the antiferromagnetic state with the same propagation vector $\boldsymbol{q} = (0\ 0\ 1/2)$ as that in $NpCoGa_5$.

Figure 1 shows the typical dHvA oscillation and the corresponding fast Fourier transform (FFT) spectrum for the magnetic field along the [001] direction. No metamagnetic transition

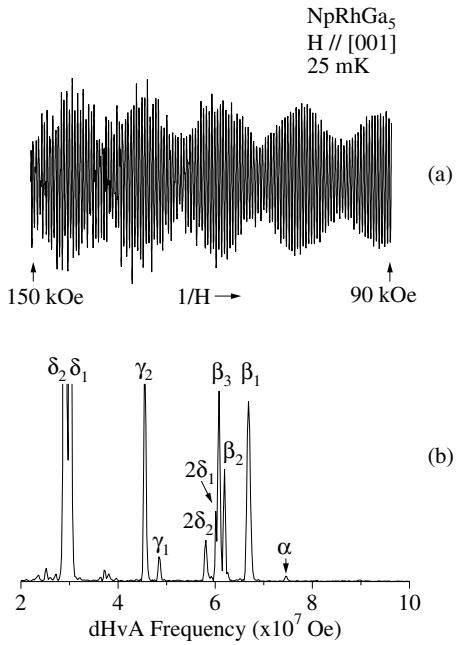

Figure 1. (a) Typical dHvA oscillation and (b) its FFT spectrum in the antiferromagnetic state of $NpRhGa_5$.

was observed in the present dHvA experiments, meaning that the measurements were done in the antiferromagnetic state. Four kinds of fundamental dHvA branches named α, β (β_1, β_2, β_3), γ (γ_1, γ_2) and δ (δ_1, δ_2), were detected, together with their harmonics of $2\delta_1$ and $2\delta_2$. Here the dHvA frequency F ($=\hbar c S_F/2\pi e$) is proportional to the extremal (maximum or minimum) cross-sectional area S_F of the Fermi surface and is expressed in magnetic field units. The subscript on the branch name δ such as δ_1 and δ_2 denotes the maximum or minimum of S_F for a corrugated Fermi surface.

We show in figure 2(a) the angular dependence of the dHvA frequency in the antiferromagnetic state of $NpRhGa_5$. The main dHvA branches α, β, γ and δ increase approximately as a function of $1/\cos\theta$ with increasing the field angle θ (θ is the tilt angle from [001] to [100] or [110]), indicating nearly cylindrical Fermi surfaces. We also detected three kinds of branches with small dHvA frequencies, named ε, ζ (ζ_1, ζ_2) and ξ.

We determined the cyclotron effective mass from the temperature dependence of the dHvA amplitude [15], as shown in table 1. The cyclotron masses of the main dHvA branches named α, β, γ and δ are in the range from 8.1 to 11.7 m_0 (m_0 is the rest mass of an electron) for $H \parallel [001]$, which are moderately enhanced, as in the similar compounds USb_2 [16], $UPtGa_5$ [17] and $CeCoIn_5$ [18], where the cylindrical Fermi surfaces are formed by the f electrons and relatively large cyclotron masses are detected.

We will compare the present dHvA results to those of energy band calculations based on the fully-relativistic spin- and orbital-polarized linear augmented-plane-wave (LAPW) method [19] within the local spin density approximation (LSDA) [20]. In the self-consistent calculations, the 5f, 6p, 6d and 7s electrons in the Np site, the 4d and 5s electrons in the Rh site and the 3d, 4s and 4p in the Ga site are treated as valence electrons. The densities and potentials are constructed in the muffin-tin approximation. The magnetic moments at the Np site are oriented antiferromagnetically along the [001] direction with $\boldsymbol{q} = (0\ 0\ 1/2)$.

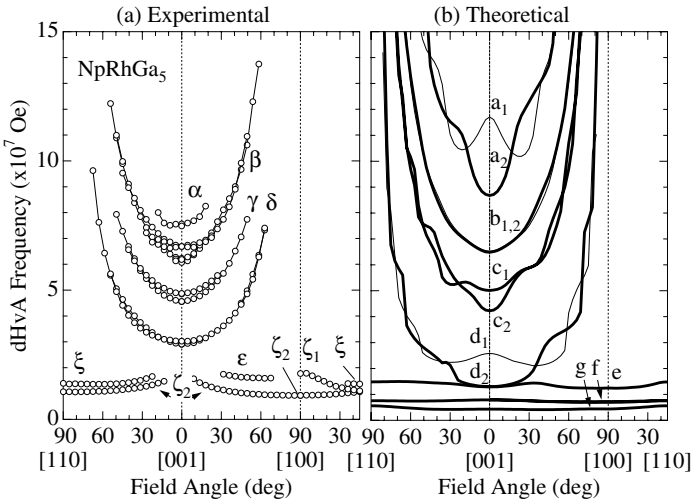

Figure 2. Angular dependence of (a) the experimental and (b) theoretical dHvA frequency in the antiferromagnetic state of $NpRhGa_5$. The thick lines in panel (b) represent the corresponding dHvA branches to the experiments, while the thin lines in panel (b) are not detected in the experiments because of the large curvature factor (see the text for details).

Table 1. Experimental dHvA frequency F, cyclotron mass m_c^*, and the theoretical dHvA frequency and band mass m_b in the antiferromagnetic state of $NpRhGa_5$.

Experimental			Theoretical		
	F ($\times 10^7$ Oe)	m_c^* (m_0)		F ($\times 10^7$ Oe)	m_b (m_0)
$H \parallel$ [001]					
			a_1	11.70	4.6
α	7.55	11.1	a_2	8.67	2.6
β_1	6.69	9.3	b_1	6.53	3.3
β_2	6.19	11.6	b_2	6.49	2.2
β_3	6.07	11.7			
γ_1	4.85	9.8	c_1	5.01	2.2
γ_2	4.55	9.0	c_2	4.22	3.3
			d_1	2.58	8.6
δ_1	3.03	10.0	d_2	1.30	2.8
δ_2	2.91	8.1			

The lattice constants a, c and the so-called z-parameter, which describes the position of the Ga atom at the 4i site $(0, 1/2, z)$ in the $HoCoGa_5$-type tetragonal structure, are set to experimental values of $a = 4.2943$ Å, $c = 6.8392$ Å and $z = 0.2987$, respectively.

The 5f bands around the Fermi energy E_F are found to be hybridized mainly with the Np-6d bands and the Ga-4p bands. The theoretical electronic specific heat coefficient γ_b was calculated as 13 mJ K^{-2} mol^{-1} from the total density of state at E_F, which is compared to the experimental value $\gamma = 52$ mJ K^{-2} mol^{-1}. The ratio γ/γ_b is 4. The contribution of the 5f electrons to the total density of states at E_F was 70%. This means that the Fermi surfaces are mainly of 5f-electron character. The spin and orbital moments at the Np site were calculated as -3.5 μ_B/Np and 4.3 μ_B/Np, respectively. The total magnetic moment is 0.8 μ_B/Np, which is in fairly good agreement with the experimental value of 0.96 μ_B/Np. Details of the energy band calculations will be published in another paper [21].

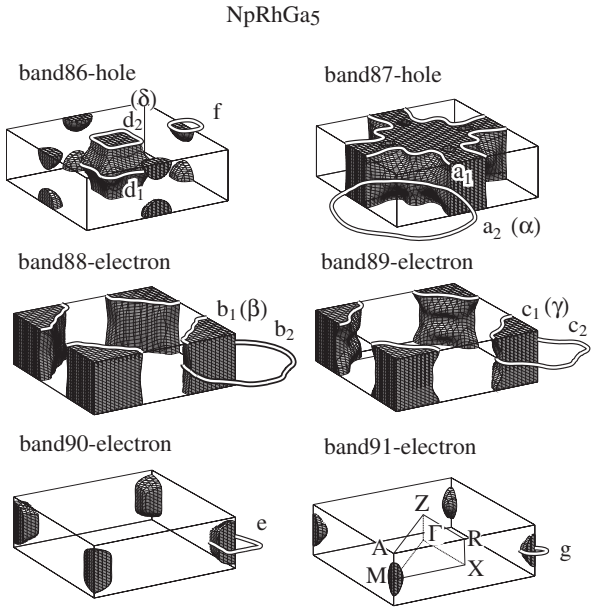

Figure 3. Theoretical Fermi surfaces in the antiferromagnetic state of $NpRhGa_5$.

We show in figure 3 the theoretical Fermi surfaces in the tetragonal Brillouin zone of the antiferromagnetic state. In the antiferromagnetic state with $\boldsymbol{q} = (0\,0\,1/2)$, the magnetic unit cell is doubled with respect to the chemical unit cell along [001], which brings about a flat magnetic Brillouin zone as shown in figure 3. All the main Fermi surfaces are nearly cylindrical, although there are three kinds of pocket Fermi surfaces named e, f and g.

The theoretical angular dependence of the dHvA frequency is shown in figure 2 (b). A comparison between experiment and theory is as follows:

(1) The experimental branch α most likely corresponds to the theoretical branch a_2, which is derived from the band 87 electron-Fermi surface centred at the M point. We note that the band 87 electron-Fermi surface is highly corrugated from a cylindrical shape, resulting that this branch splitting largely into the maximal cross-sectional area a_1 and the minimal cross-sectional area a_2 for $H \parallel [001]$. For branch a_1, the curvature factor $|\partial^2 S_F/\partial {k_z}^2|^{-1/2}$, which is proportional to the dHvA amplitude [15], is very unfavourable for detecting the dHvA signal. Therefore the dHvA branch corresponding to the branch a_1 was not detected experimentally.

(2) The experimental branches β and γ are in good agreement with the theoretical branches $b_{1,2}$ and c_1 (c_2), respectively, which correspond to the cylindrical shapes of bands 88 and 89 electron-Fermi surfaces centred at the M point, respectively, as shown in figure 3. If we assume that the experimental branches β and γ are due to perfect cylindrical Fermi surfaces, the corresponding Fermi surfaces occupy 29 and 21% of the antiferromagnetic Brillouin zone, respectively, in total 50%.

(3) The experimental branch δ corresponds to the theoretical branch d_2, which is derived from the band 86 hole-Fermi surface with the corrugated cylindrical shape centred at the Γ point. The theoretical dHvA frequency of branch d_2 is, however, smaller than the experimental frequency of branch δ in magnitude. The theoretical branch d_1 was not

detected experimentally, for the same reason as for branch a_1. Otherwise the exact Fermi surface is not corrugated but is cylindrical.

(4) In addition to these main Fermi surfaces, we detected three kinds of dHvA branches with small dHvA frequencies named ε, ζ_1 (ζ_2) and ξ, which might correspond to theoretical ones named e, f and g, respectively, although these dHvA branches were not detected experimentally in the whole angle region.

The ratio of the cyclotron mass to the band mass m_c^*/m_b is in the range from 5.3 to 2.7, which is fairly consistent with the ratio $\gamma/\gamma_b = 4$ mentioned above.

Next we will compare the Fermi surfaces of $NpRhGa_5$ to those of $NpCoGa_5$ and $UPtGa_5$. The dHvA results of $NpRhGa_5$ should be similar to those of $NpCoGa_5$ in the antiferromagnetic state, namely below H_m, because of the similar magnetic structure with $\boldsymbol{q} = (0\,0\,1/2)$ and the same number of the valence electrons. In fact, branch ζ_1 (ζ_2) in $NpRhGa_5$ displays a similar angular dependence in $NpCoGa_5$ [6]. The main dHvA branches in $NpRhGa_5$, which correspond to branches α, β, γ and δ in figure 2(a), were, however, not detected in $NpCoGa_5$, because magnetic fields below $H_m = 43$ kOe, which preserve the antiferromagnetic state, are not large enough to detect the dHvA oscillations in $NpCoGa_5$.

Four kinds of cylindrical Fermi surfaces in $NpRhGa_5$ might, however, be simply speculated from the two kinds of cylindrical Fermi surfaces observed in the field-induced ferromagnetic state of $NpCoGa_5$, as a result of the band-folding procedure, because the Brillouin zone in the antiferromagnetic state is reduced to half of the Brillouin zone in the field-induced ferromagnetic state along [001].

It is also useful at present to consider the previous dHvA results of the similar antiferromagnetic compound $UPtGa_5$. $UPtGa_5$ orders antiferromagnetically with the propagation vector $\boldsymbol{q} = (0\,0\,1/2)$ [22], which is the same as that of $NpRhGa_5$. The total number of valence electrons in $UPtGa_5$ (U ($5f^3 6d^1 7s^2$), Pt ($5d^9 6s^1$) and Ga ($4s^2 4p^1$)) is also the same as that in $NpRhGa_5$ (Np ($5f^4 6d^1 7s^2$), Rh ($4d^8 5s^1$) and Ga ($4s^2 4p^1$)) on the basis of the 5f-itinerant band picture, where in $NpRhGa_5$ the 5f electrons of Np are larger by one and the d electrons of Rh are smaller by one in number, compared to the valence electrons in $UPtGa_5$. In the dHvA experiments of $UPtGa_5$ [17], similar four kinds of cylindrical Fermi surfaces were detected in the antiferromagnetic state. These Fermi surfaces were approximately explained by the result of similar energy band calculations. We note that the calculated Fermi surfaces are more corrugated than the experimental ones in $UPtGa_5$. There is a similar tendency in $NpRhGa_5$.

$NpCoGa_5$, $NpRhGa_5$ and $UPtGa_5$ mentioned above are antiferromagnets. On the other hand, $PuCoGa_5$ and $PuRhGa_5$ possess no magnetic ordering, but exhibit superconductivity at low temperatures. The 5f-localized character is, however, reflected in the high-temperature magnetic susceptibility [1, 2]. These characteristic features in $PuCoGa_5$ and $PuRhGa_5$ are similar to those of $CeCoIn_5$ with a superconducting temperature $T_c = 2.3$ K [23]. The topology of the Fermi surface in $CeCoIn_5$, observed by the dHvA experiments, was well explained by the 5f-itinerant band model [18]. There is still the need to clarify the Fermi surface properties of $PuCoGa_5$ and $PuRhGa_5$ via dHvA experiments, which are left to a future study. The present experimental and theoretical dHvA results of $NpRhGa_5$, together with those of $UPtGa_5$ and $CeCoIn_5$, are useful in a systematic understanding of the f electrons.

We summarize the present dHvA results of the transuranium antiferromagnetic compound $NpRhGa_5$. In the dHvA experiments for $NpRhGa_5$, we detected four kinds of nearly cylindrical main Fermi surfaces. These Fermi surfaces are well explained by the result of the spin- and orbital-polarized energy band calculations based on the 5f-itinerant band model. The present

result is the first case in transuranium compounds where the 5f electrons play a role of the magnetic moment and also significantly contribute to the volume of the Fermi surface.

We thank N Metoki and J Flouquet for fruitful discussion. This work was financially supported by the Grants-in-Aid for Scientific Research (A), (C), Young Scientists (B), Scientific Research on Priority Areas and Creative Scientific Research (15GS0213) from the Japan Society for the Promotion of Science.

References

[1] Sarrao J L *et al* 2002 *Nature* **420** 297
[2] Wastin F *et al* 2003 *J. Phys.: Condens. Matter* **55** S2279
[3] Maehira T *et al* 2003 *Phys. Rev. Lett.* **90** 207007
[4] Opahle I and Oppeneer P M 2003 *Phys. Rev. Lett.* **90** 157001
[5] Aoki D *et al* 2004 *J. Phys. Soc. Japan* **73** 519
[6] Aoki D *et al* 2004 *J. Phys. Soc. Japan* **73** 2608
[7] Aoki D *et al* 2005 at press
[8] Honda F *et al* 2005 at press
[9] Colineau E *et al* 2004 *Phys. Rev.* B **69** 184411
[10] Metoki N *et al* 2005 at press
[11] Aoki D *et al* 2004 *J. Phys. Soc. Japan* **73** 1665
[12] Colineau E *et al* 2005 *J. Alloys Compounds* **386** 57
[13] Jonen S *et al* 2005 at press
[14] Shiokawa Y *et al* 1996 *J. Alloys Compounds* **255** 98
[15] Ōnuki Y and Hasegawa A 1995 *Handbook on the Physics and Chemistry of Rare Earths* vol 20, ed K A Gschneidner Jr and L Eyring (Amsterdam: Elsevier Science) p 1
[16] Aoki D *et al* 2000 *Phil. Mag.* B **80** 1517
[17] Ikeda S *et al* 2003 *J. Phys. Soc. Japan* **72** 576
[18] Settai R *et al* 2001 *J. Phys.: Condens. Matter* **13** L627
[19] Yamagami H 2000 *Phys. Rev.* B **61** 6246
[20] von Barth U and Hedin L 1972 *J. Phys. C: Solid State Phys.* **5** 1629
[21] Yamagami H 2005 at press
[22] Tokiwa Y *et al* 2002 *J. Phys. Soc. Japan* **71** 725
[23] Petrovic C *et al* 2001 *J. Phys.: Condens. Matter* **13** L337